
Modern morpho-sedimentological patterns in a tide-dominated estuary system: the Bay of Brest (west Brittany, France)

Gregoire Gwendoline ^{1,2,*}, Ehrhold Axel ², Le Roy Pascal ¹, Jouet Gwenael ², Garlan Thierry ³

¹ Institut Universitaire Européen de la Mer, Plouzané, France

² IFREMER, Géosciences Marines, Centre de Brest, Plouzané, France

³ SHOM, Centre Hydrographique, Brest, France

* Corresponding author : Gwendoline Gregoire, email address : gwendoline.gregoire@ifremer.fr

axel.ehrhold@ifremer.fr ; pascal.leroy@univ-brest.fr ; gwenael.jouet@ifremer.fr ; Thierry.garlan@shom.fr

Abstract :

Long-studied with respect to its sedimentological features (1897), the Bay of Brest (Western Brittany, France) is a textbook example of a tide-dominated estuary. Characterised by macrotidal conditions, this estuary system is sheltered from the open sea (Iroise Sea) by a narrow strait that partitions the wave tide influences and continental/marine inputs. Sediments are supplied to the bay both by rivers (the Aulne and Elorn rivers) and by marine tidal currents. This study presents new analyses of detailed facies and morphological patterns, based on the integration of multisource data compiling seabed sampling, swath and LIDAR bathymetry, and backscatter imagery. The Main Map, at a scale of 1:90,000, contains (1) a sedimentological distribution using the 'Code Manche' classification, (2) a morphological map, and (3) bathymetric mapping which presents the morphology of marine and terrestrial landforms. This work may lay the foundation for a future study on sedimentary transport in a unique and confined coastal environment.

Keywords : Morpho-sedimentological cartography, tide-dominated, estuary system, estuarine sedimentation, backscatter imagery, Bay of Brest

1. Introduction

According to the definition by Dalrymple, Zaitlin and Boyd (1992), tide-dominated estuaries are characterised by funnel shaped morphologies and highly dynamic environments dominated by strong tidal currents, with lesser influence from waves and river currents. Numerous studies have been devoted to these environments in recent years and the morphology and sedimentary partitioning of tide-

dominated estuaries are predictable in general terms (Davis and Hayes, 1984; Dalrymple, Knight, Zaitlin, & Middleton, 1990; Dalrymple & Zaitlin 1994; Dalrymple, Mackay, Ichaso, & Choi, 2012; Tessier, Delsinne, & Sorrel, 2010; Ryan et al., 2007). At the estuary entrance, the accelerated tide currents shape the seafloor into many bedforms such as dune fields as observed in the San Francisco Bay (Barnard, Erikson, Elias & Dartnell, 2012) or large scours features as reported in the Minas Basin in the Bay of Fundy (Shaw, Todd & Li, 2014). The gradual decrease in current intensity allows sediments to deposit in sheltered areas. Nevertheless, not much is known about the detailed facies and the patterns of morphological changes controlling the balance between erosion and sedimentation. This knowledge is essential for understanding the sedimentary exchanges between continental and marine domains and is of utmost importance in deciphering human influence from natural controls. The Bay of Brest offers us the opportunity to examine these points and to compare them with previous studies. Located at the western-most part of Brittany (France) it is a large tide-dominated estuary system (about 230 km²) with macrotidal conditions. The estuary system is sheltered from the open sea (Iroise Sea) by a narrow, one nautical mile wide, strait (the *Goulet*) formed of Brioverian (end of Precambrian) rocks and controlled by an inherited Hercynian fault system. This N70°E trending fault system separates two regional geological domains composed of Hercynian granitic rocks to

49 the North of the main fault and sedimentary rocks to the south (Brioverian and Paleozoic) which
50 form the whole rocky basement of the bay (Babin, Didier, Moign, & Plusquellec, 1969; Ballèvre,
51 Bosse, Ducassou, & Pitra, 2009; Ballèvre et al., 2014; Garreau, 1980). The strait corresponds to a
52 relatively enclosed channel (about 60m below sea level) where tidal currents are subjected to
53 venturi effect and reach speeds up to 9m/s during spring tides. This allows the exchange of about
54 700×10^6 to 1×10^9 m³ of seawater at each tidal cycle which corresponds to about the third of the
55 mean water volume of the bay (Fichaut, 1984). The strait also marks the transition between 1) the
56 oceanward extension of the estuary system to the west which can be dominated by the swell
57 mostly during south-west storm events and 2) a large (180 km²) semi-enclosed bay to the east (the
58 Rade de Brest *s.s.*). In this last internal domain, wave action has a limited influence and marine
59 hydrodynamics are clearly dominated by tidal currents ranging from 0.25 to 2 m/s (SHOM,
60 1994). Sediments are supplied to the bay both from continental sources, fed by two main rivers
61 (Aulne and Elorn) with a total annual load of about 1×10^4 T, and marine sources due to the flood
62 currents (Auffret, 1983; Bassoulet, 1979). The first sedimentary map of the Bay of Brest,
63 published in 1897, by the French hydrological department (SHOM) is believed to be one of the
64 oldest representative map in the world (*in* Garlan, 2012). Successive works devoted to studying
65 the sedimentation of the bay were based on interpolation of sediment sampling over time
66 (Auffret, 1983; Fichaut, 1984; Guérin, 2004; Guilcher & Pruleau, 1962; Hallégouët, Moign &
67 Lambert, 1979; Hirschberger, Guilcher, Pruleau, Moign & Moign, 1968; Moign, 1967). In this
68 study, a new sedimentary map is made based on integration of multisource data combining
69 seabed sampling, with bathymetric data collected by the SHOM and the French Institute for
70 marine studies (IFREMER), with the integration of surveys conducted for the benthic fauna
71 habitat mapping program (REseau BENThique, Ehrhold, Hamon & Guillaumont, 2006) by the
72 European Institute for Marine Studies (IUEM). Additional side-scan backscattering imagery
73 based on interferometry sonar conducted by IFREMER was also used to evaluate the nature of

74 the seabed. Using this, geomorphic and sedimentary maps are presented to highlight the type of
75 sediment characterising the different depositional environments through the estuary system.

76 **2. Methods**

77 ***2.1 Geomorphological analysis***

78 The bathymetric map was created by processing and interpolating data from multibeam
79 echosounder surveys for the deepest domains (from 10 m to 50 m in Lower Astronomical Tide
80 L.A.T) and from aerial LIDAR (Light Detection and Ranging) for the shallowest part (from land
81 to 10 m in LAT). Data provided from five geophysical surveys (Rebent 14, 17, 20, 2013 and
82 Esstech) were compiled to obtain the deepest bathymetry of the marine landform map. Swath
83 bathymetry data were mainly acquired on board the *R/V La Thalia* using the *Simrad EM 1000*
84 and *EM 2040* multibeam systems, working at frequencies of 93-98 kHz and 200-400 kHz,
85 respectively. The intermediate deep waters were surveyed by the launch *Haliotis*, equipped with
86 an interferometric system Geoacoustics Geoswath, working at a frequency of 250 kHz. Data
87 processing was performed using *Caribes* subsea mapping software developed by IFREMER,
88 which included the correction of attitude sensor data (roll, pitch, and heave), the application of
89 sound velocity profiles and tide corrections, and the use of statistical and geometrical filters to
90 remove any unorganised noise. Processed data were gridded in order to obtain diverse Digital
91 Terrain Models with cell-size varying from 1 m to 50 m of resolution. The laser detection or
92 LIDAR, acquired by plane, is provided by the SHOM and IGN (© Litto3D) using the French
93 altimeter system IGN69 with a resolution of 1 m. These data were converted in LAT with
94 ARCGIS (© ESRI) and Circee (© IGN) software. For the emerged part, data were obtained
95 from the I.G.N (Institut Geographique National) with an elevation reference in NGF93. Surveys,
96 LIDAR, and continental elevation grid data were merged using the FLEDERMAUS (© IVS)
97 software to a resolution of 5 m. The identification and mapping of geometric features was carried

98 out using ARCGIS software with a variety of resolution grids (1-5 m) in order to be able to the
99 differentiate the features at different scales.

100 ***2.2 Backscattering imagery and Sedimentological analyses***

101 The sidescan sonar signatures result from backscatter variation (imagery) that depends on the
102 seabed material and it is macro-morphology (Augustin et al., 1996; Augustin & Lurton, 2005;
103 Lamarche, Lurton, Verdier, & Augustin, 2011; Le Chenadec, Boucher, & Lurton, 2007; Lurton,
104 2003). Their identification relies on the interpretation of shades of grey and apparent textures in
105 the mosaic. The ensuing geological interpretation of the area requires correlations between
106 surficial sediment characteristics and the mosaic backscatter interpretation, and thus depends on
107 ground-truth. Accordingly, 148 samples were analysed by the sieving method: sediments were
108 passed through sieve columns of different sizes [Figure 1]. Fourteen sieves of square mesh were
109 used in order to characterise the grain size repartition for the heterogeneous sediment (25,000 μm
110 to 40 μm) [Figure 1]. The wet sieving method was used for the finest samples along with a *Coulter*
111 *LS200* diffraction laser microgranulometer. Carbonate content was measured with a Bernard
112 calcimeter using the volumetric calcimetric method. Both analyses allowed us to define 19
113 sediment types in the *Manche Code* classification adopted for English Channel sedimentological
114 mapping (Larsonneur, Bouysse & Auffret, 1982).

115 [Figure 1 near here]

116 The final sedimentary map produced by the correlation between backscatter imagery facies and
117 the dominant sediment type-class allowed us to establish a reference nomenclature for domains
118 of the study area – such as external, internal, estuaries – to be applied to the whole bay [Figure 1
119 and 3].

120 **3. Results and interpretation**

121 The new morpho-sedimentological map highlights the partitioning of the estuary system study in
122 three main areas [Figure 3]: (1) A western outer domain open to the ocean (Iroise Sea); (2) An
123 intermediate domain comprising the *strait* and extending toward the bay until a virtual line joining
124 the *Longue* and *Ronde* islands; and (3) An inner domain characterised by the benches, tidal flats,
125 and coastal river mouths (Aulne, Elorn and Daoulas rivers).

126 ***3.1 Morphological description***

127 The main morphological features are the presence of a well-marked channel network spread out
128 along the seafloor and extended bench/tidal flat covering more than half of the surface of the
129 bay and started on both sides of the channel.

130 [Figure 2 near here]

131 The channels extend from the coastal river mouths and incises the Palaeozoic basement of the
132 bay. They correspond to fluvial paleo-valleys formed during successive Quaternary sea level
133 lowstands (Hallégouët, 1994) and evolved as tidal inlets after the settling of the present-day high
134 sea-level. In the vicinity of the river mouths, the thalwegs of the paleo-valleys are narrow (500
135 meters) and are V-shaped with a depth ranging from 20 to 25 meters below sea-level
136 (b.s.l.) [Figure 2]. The channel geometries evolved in relation with the bedrock geology and differ
137 between the two channel systems related to the two rivers Aulne and Elorn. For this last one, the
138 relatively straight channel, oriented from the NE to the SW, is clearly controlled by the regional
139 Elorn fault system, while the NW trending Aulne estuary meanders further thanks to the
140 sedimentary basement. The channels appear discontinuous at several places with the
141 individualisation of 'blind' tidal channels. The origin of this discontinuity seems more linked to
142 the structural control of the fluvial paleo-valleys rather than process of dichotomy of tidal
143 channels as described for estuaries (Robinson, 1960). Along the meanders, the channels widen
144 (1500 meters) and paleo-terraces are visible on both sides with depth of 20 m b.s.l to the south

145 rim and 15 m b.s.l. to the north. Both channels converge at the centre of the bay to form a main
146 paleo-valley connected to the deep strait extending to the external domain. Here, the U-shape
147 channel tightens and is bounded by abrupt cliffs [Figure 2]. At the *goulet* end, the thalweg shows a
148 large 750 m wide flat bottom and preserves its abrupt rim to the North. In the central part of the
149 external area the vein widens and becomes shallowest before tightening in the most downstream
150 portion of the system [Figure 2].

151 Sedimentary bedforms are mostly established in the external and intermediate domains. Long
152 NE-SW trending tidal sand ridges are located at each termination of the strait and along the main
153 channel of the central part of the bay. Most of them appear linked to the presence of residual
154 current eddies generated by the tidal flow upon entry in the bay and are therefore considered to
155 be representative of banner sand ridges (Davis & Balson, 1992, Dyer & Huntley, 1999, Neill &
156 Scourse, 2009).

157 The most significant of them is the *Cormorandière* ridge (length: 1.8 km, width: 0.8 km, height: 3
158 m) extending to the east of the *Espagnols* headland and occurring along the western rim of a
159 channel segment. In the external domain there is a banner bank found in the *Capucine* headland
160 from the NE to SW, while dunes and megaripple fields have been identified in the paleo-valley.
161 Rippled scour depressions (RSD) that are “channel-like depressions of low, negative relief [...],
162 containing large sand ripples” (Cacchione, Drake, Grant, & Tate, 1984) are observed on the shelf
163 surrounding the channel at depths between 20 and 10 meters (b.s.l). Off the bay of Bertheaume,
164 the RSDs are formed from bedrock outcrop and they extend about 4,500 meters towards the
165 NNE. They are characterised by an alternation of negative relief furrows, containing symmetric
166 and regular ripples following the same orientation, and positive relief bands of a similar width. In
167 the south, RSDs cover the main part of the Bay of Camaret and form a large depression filled by
168 symmetric and regular ripples oriented towards the SSE. A megaripple field occurs in the central
169 part of the external domain where the thalweg is the widest and presents many types of features

170 characterised by different wave length, symmetry, and orientation. Dunes cover the north rim of
171 the thalweg at the exit of the *goulet* and are oriented towards the NE.

172 ***3.2 Sedimentological description***

173 To complete the morphological analysis, the sedimentological map is divided into three main
174 areas corresponding to the geomorphologic domains.

175 [Figure 3 near here]

176 The external domain is characterised by contrasting sediments between the north and south side
177 of the main channel. The northern part is defined by a shelf where the RSDs formed by gravelly
178 coarse sand are inserted in an alternation of shelly sandy stripes ranging from coarse gravelly sand
179 to fine sand [Figure 3]. The channel limit on the south side is defined by the last strip of medium
180 sand, while the megarippled field is constituted by fine sand and the dunes by shelly gravelly
181 coarse sand. Beyond this limit the sedimentary repartition is more heterogeneous. The south area
182 is composed of coarse lithoclastic sediment (gravelly sand to pebble) occasionally mixed with a
183 finer matrix, as in the example of the slight depression (40 meters) in the western part where
184 coarse grains are associated with at least 5% mud [Figure 3]. The intermediate domain and the
185 *goulet* collects the coarser sediments, most of 30% is composed of outcrops surrounded by
186 pebbles stemming from the erosion of the nearby sedimentary rocks or gelivation (schist
187 plaques). Some places are coated by a thin cover of shelly gravelly coarse sand [Figure 3]. In the
188 central part of the Bay of Brest, deposits from the central outcrops become finer until the *Ronde*
189 *Island*. However the *Cormorandière* bank cover is locally formed by shelly sandy gravel and has
190 disrupted the grain size sorting [Figure 3].

191 A muddy fraction characterises the estuarine domain; all the benches and tidal flats are covered
192 by mixed sediments containing a more and less concentrated matrix of mud [Figure 3]. Two main
193 types of sediment characterised by the mud content are observable: the muddy sediments that
194 contain a minimum 25% mud (blue in the map) and sediments that contain between 5 and 25%

195 mud (green in the map). The concentration increases around estuaries mainly in the Elorn and
196 Daoulas river mouths. In this study this difference is assumed to be induced by the presence of
197 macrobenthic communities composed mainly of shells (*Crepidula*) and maërl, whose
198 development has provided the coarse fraction of the sediment (Grall & Hall-Spencer, 2003;
199 Hirschberger, Guilcher, Pruleau, Moign & Moign, 1968) [Figure 3].

200 ***3.3 Sediment dynamics interpretation***

201 The estuarine internal domain is characterised by shallow benches and tidal flats that are covered
202 by mud inputs principally fed by the Aulne River (Bassoulet, 1979; Beudin, 2014). The marine
203 fauna and flora species development indicates that the turbidity is relatively low and that currents
204 are moderate (Grall & Hily, 2002). Thus, this estuarine domain has a sedimentary partitioning
205 mainly controlled by the continental fluvial inputs that are weakly reworked after the sediment
206 deposits. In the intermediate domain, the many outcrops reflect the strong intensity of tidal
207 currents preventing the sedimentary deposits. The tidal sand ridges located in the centre of the
208 main channel seem to be an indication of confrontation between ebb and flux currents, and
209 decreasing grain size sorting deposits in the central part of the bay reveal the reduction in tidal
210 current speed. In the outer domain the dune and megaripple fields, characterised by a gravelly
211 shelly sand, reflect the impact of the tidal currents. The presence of rippled scour depressions,
212 including symmetric megaripples, suggests that sedimentation in the outer area is more affected
213 by the swells oriented principally in the same direction as these structures (Auffret, Augris,
214 Cabioch, & Koch, 1992; Mazières et al., 2015). Finally, the patch of muddy sediment in the
215 western part is interpreted as a “sink” depositional area where the continental muddy sediments
216 sourced from the Bay of Brest may be deposited and this deepest portion of the basin should
217 have been spared the effect of swell except in case of exceptional storms.

218 **Conclusion**

219 The refined high-resolution morpho-sedimentological map of the Bay of Brest combining
220 sediment sampling, bathymetry, and backscatter imagery allows us to provide a new accurate

221 mapping of the sedimentary partitioning in accordance with seabed morphology analysis. It
222 highlights the detailed facies distribution and morphology patterns useful for understanding the
223 estuary processes and aids characterisation of the hydrodynamic conditions occurring in the open
224 sea and confined domains. It appears that the Bay of Brest *s.s.*, should be categorised as confined
225 estuary controlled by tidal currents in the deep water areas, which preserve the inherited shape
226 and terraces associated with paleo-valley activity during successive sea-level lowstands, and by the
227 fluvial inputs in the most remote shallowest area. The external domain is controlled both by tidal
228 currents with the main stream canalized in the paleo-valley and by the Atlantic swell affecting the
229 large exposed shelves where the depth is less profound. The resulted map illustrates the main
230 hydrodynamic processes which impact the sediment distribution at the land-sea transition.
231 Several studies have already used the methods presented in this paper to understand the dynamics
232 processes impact in the geomorphology and sedimentary partitioning in a tide dominated
233 estuaries (Barnard, Erikson, Rubin, Dartnell & Kvitek, 2012; Barnard, Erikson, Elias & Dartnell,
234 2012; Garcia-Gíl, Durán & Vilas, 2000; Shaw, Todd & Li, 2014). This new study will allow
235 detailed comparison of scale facies distribution with other confined estuaries. Further modelling
236 will allow the quantification of these processes and estimation of their relative contribution to the
237 finer-grain sedimentation in the well-constrained geomorphology of an original estuary system.

238 **Software**

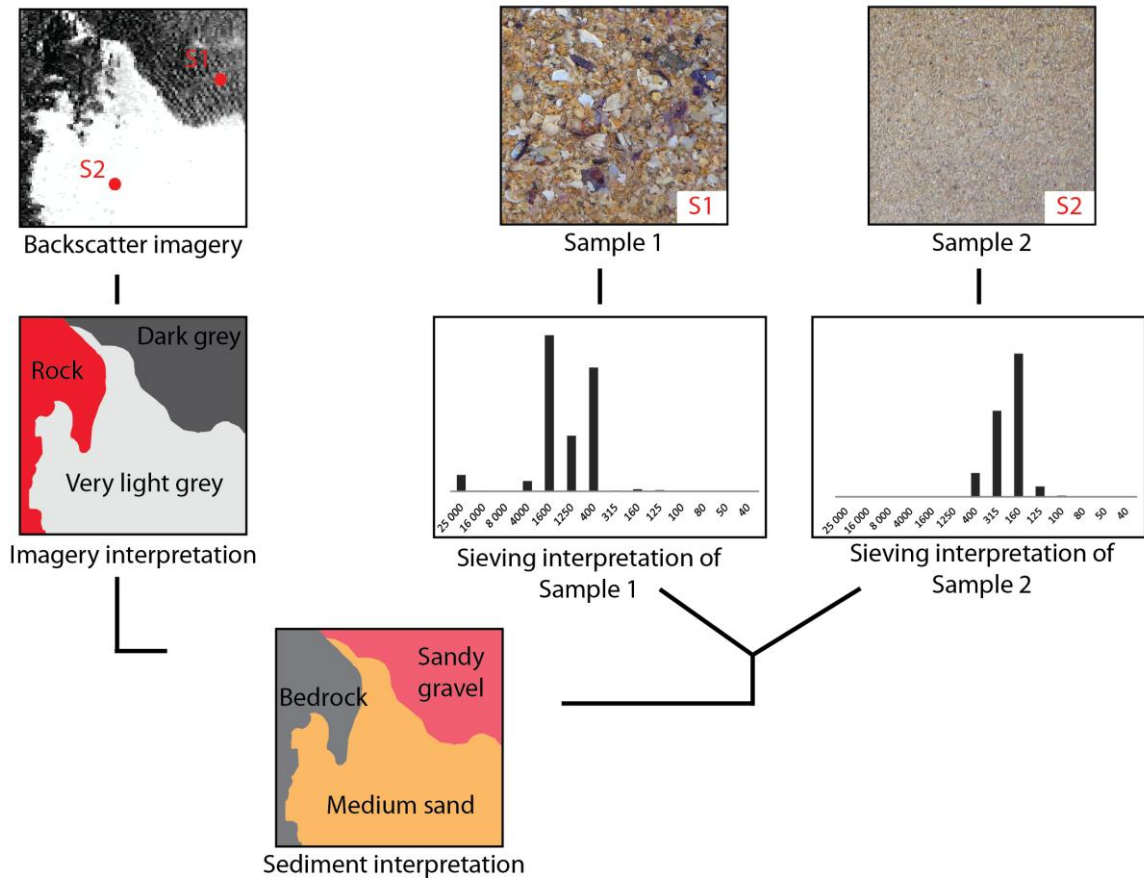
239 ESRI ArcMap 10.2 software was used for digitising backscatter variation and sediment type-class.
240 Fledermaus and Circee[®] were used to create the bathymetric map. Map layout and final editing
241 was performed using Adobe Illustrator CS5.

242 **Acknowledgements**

243 The authors acknowledge financial support by Labex Mer and the Brittany Region. We would
244 like to thank IFREMER, in particular the organizer of the Rebent program, and the University of
245 Western Brittany (UBO), for collecting data. We would like to thank SHOM and IGN for
246 providing the LIDAR data (litto3D[©]). We would also like to thank the boarding staff and

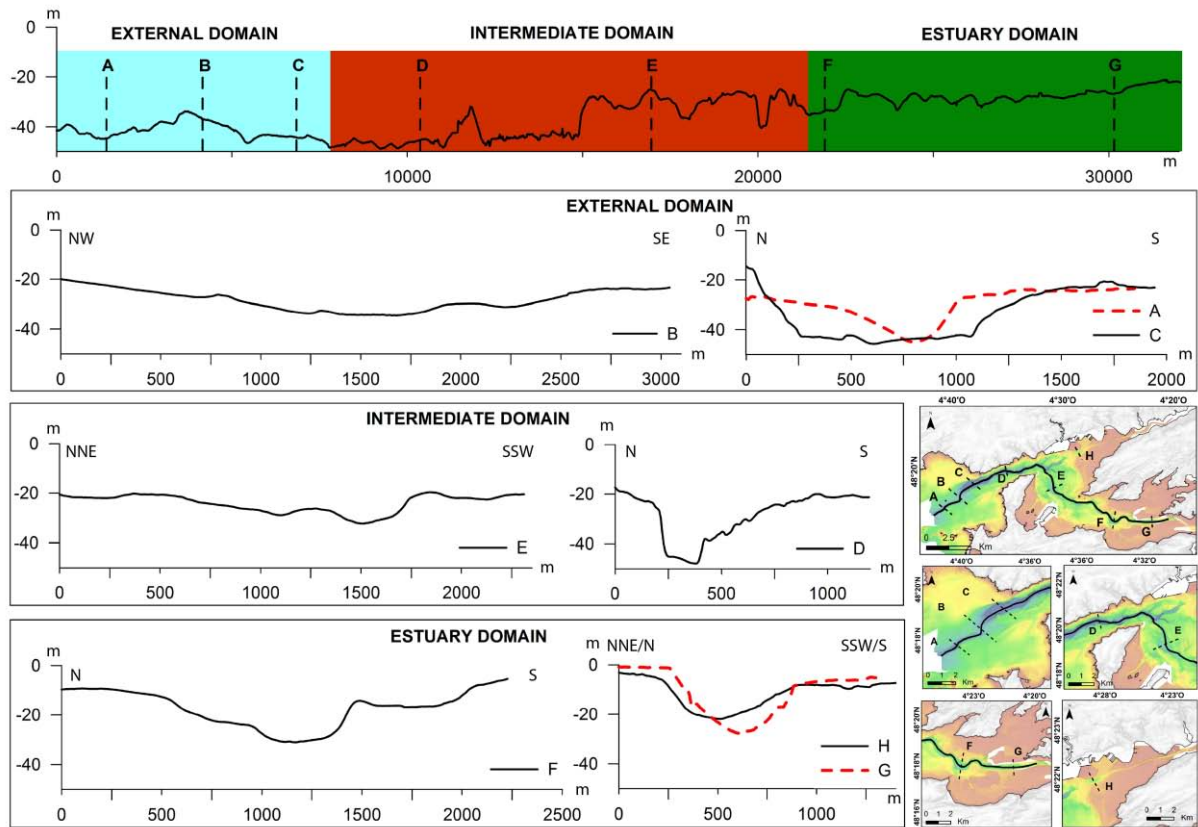
247 technicians. The authors are very grateful to Chris Orton, to Luisa Sabato, to Thomas S.N. Oliver
 248 and the associate editor Wayne Stephenson for their careful examination of previous versions of
 249 this paper and for their helpful comments.

250 **Figures**



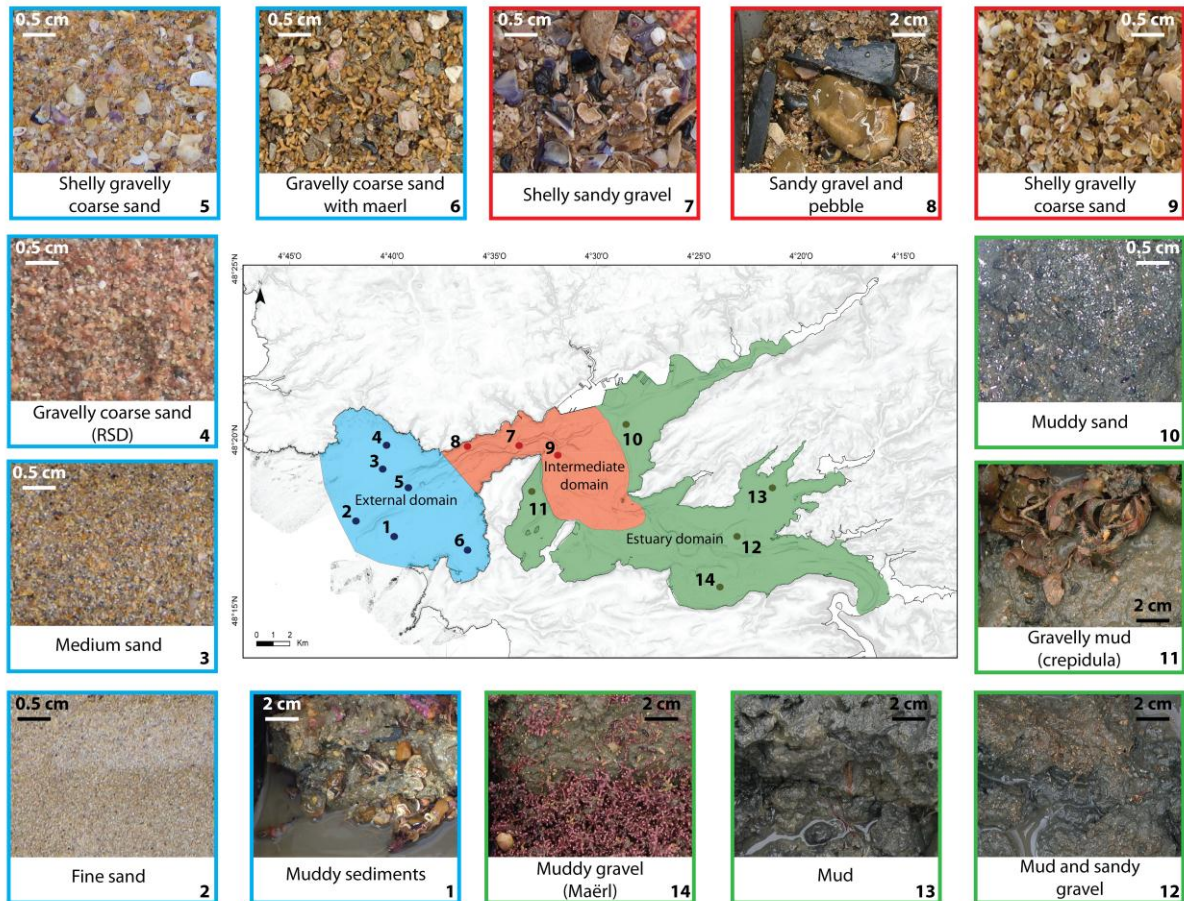
251

252 Figure 1 : Methods for the creation of the sedimentological map of the Bay of Brest: In the left
 253 top corner the side scan sonar (1:5,000) analysis allowed us to define the backscatter variations
 254 (grey nuances); in the right top, sample analysis by the sieving method is translated into a
 255 histogram for each sieve and shows the final sedimentary interpretation.



256

257 Figure 2: Shape of the paleo-footprints and their localisation on the maps on the right lower
 258 corner (scale of 1:90,000 and 1:30,000). On the top this is the profile that follows the channel
 259 from the Iroise Sea to the Aulne estuary divided in three main domains: external (blue),
 260 (intermediate (red), estuary (green); shapes of each domain are illustrated.



261

262 Figure 3 : The location of three main domains of the study area and facies samples; the external
 263 domain (in blue) is characterised by sand (fine to gravelly) and shelly sand, the gravelly coarse
 264 sediment located in the RSD (Ripple Scour Depression) is observable for the north and south;
 265 the intermediate domain (in red) by shelly sandy gravel and pebbles; the external domain (in
 266 green) defined by mud mixed in different proportions with other calcareous sediments like
 267 crepidula of maërl.

268 References

269 Allen, G. P. (1991). Sedimentary processes and facies in the Gironde estuary: a recent model for
 270 macrotidal estuarine systems. In: *Clastic Tidal Sedimentology* (Ed. by D.G Smith, G.E Reinson, B.A
 271 Zaitlin and R.A Rahmani), pp.29-40. Canadian Society of Petroleum Geologists, 16.

272 Auffret, G. A. (1983). *Dynamique sédimentaire de la marge continentale celtique-Evolution Cénozoïque-*
 273 *Spécificité du Pleistocène supérieur et de l'Holocène* (Doctoral dissertation), Université de Bordeaux I,
 274 Bordeaux.

- 275 Auffret, J. P., Augris, C., Cabioch, L., & Koch, P. (1992). Sillons graveleux aux abords de la Baie
276 de Morlaix [Furrows gravel near the Bay of Morlaix]. *Ann. Soc. Geol. Nord*, 1, 143-147. Retrieved
277 from https://scholar.google.fr/scholar?q=auffret+1992+augris&btnG=&hl=fr&as_sdt=0%2C5
- 278 Augustin, J. M., Le Suave, R., Lurton, X., Voisset, M., Dugelay, S., & Satra, C. (1996).
279 Contribution of the multibeam acoustic imagery to the exploration of the sea-bottom. *Marine*
280 *Geophysical Researches*, 18(2-4), 459-486.
281 doi: 10.1007/BF00286090
- 282 Augustin, J. M., & Lurton, X. (2005). Image amplitude calibration and processing for seafloor
283 mapping sonars. In *Oceans 2005-Europe, IEEE*, 1, 698-701.
284 doi: 10.1109/OCEANSE.2005.1511799
- 285 Babin, C., Didier, J., Moign, A., Plusquellec, Y. (1969). Goulet et rade de Brest : Essai de géologie
286 sous-marine [Goulet and bay of Brest : Submarine geology test]. *Revue de géographie physique et de*
287 *géologie dynamique*, XI(2), 55-63.
288 Retrieved from [http://etudes.bretagne-](http://etudes.bretagne-environnement.org/index.php?lvl=notice_display&id=15957)
289 [environnement.org/index.php?lvl=notice_display&id=15957](http://etudes.bretagne-environnement.org/index.php?lvl=notice_display&id=15957)
- 290 Ballèvre, M., Bosse, V., Ducassou, C., & Pitra, P. (2009). Palaeozoic history of the Armorican
291 Massif: models for the tectonic evolution of the suture zones. *Comptes Rendus Geoscience*, 341(2),
292 174-201.
293 doi: 10.1016/j.crte.2008.11.009
- 294 Ballèvre, M., Catalán, J. R. M., López-Carmona, A., Pitra, P., Abati, J., Fernández, R. D., ... &
295 Martínez, S. S. (2014). Correlation of the nappe stack in the Ibero-Armorican arc across the Bay
296 of Biscay: a joint French–Spanish project. *Geological Society, London, Special Publications*, 405(1), 77-
297 113.
298 doi: 10.1144/SP405.13
- 299 Barnard, P.L., Erikson L.H, Rubin, D., Dartnell, P. & Kvittek, R.G. (2012). Analyzing bedforms
300 mapped using multibeam sonar to determine regional bedload sediment transport patterns in the
301 San Francisco Bay coastal system. Sedimentology. In: *Sediments, Morphology and Sedimentary Processes*
302 *on continental shelves : Advances in technologies, research and application* (Ed. by M.Z., Li, C.R., Sherwood
303 and P.R., Hill), pp. 273-294. Special Publication of the International Association of
304 Sedimentologists (IAS), 44.
- 305 Barnard, P.L, Erikson, L.H., Elias, E.P.L., & Dartnell, P. (2012). Sediment transport patterns in
306 the San Fransisco Bay coastal system from cross-validation of bedform asymmetry and modelled
307 residual flux. *Marine Geology*, 345, 72-95.
308 doi: 10.1016/j.margeao.2012.10.011
- 309 Bassoulet, P. (1979). *Etude de la dynamique des sédiments en suspension dans l'estuaire de l'Aulne: Rade de*
310 *Brest* (Doctoral dissertation). Université de Bretagne occidentale, Brest.
- 311 Beudin, A. (2014). *Dynamique et échanges sédimentaires en rade de Brest impactés par l'invasion de crépidules*
312 (Doctoral dissertation). Université de Bretagne Occidentale, Brest.

- 313 Cacchione, D. A., Drake, D. E., Grant, W. D., & Tate, G. B. (1984). Rippled scour depressions
314 on the inner continental shelf off central California. *Journal of Sedimentary Research*, 54(4), 1280-
315 1291. Retrieved from [http://archives.datapages.com/data/sepm/journals/v51-
316 54/data/054/054004/1280.htm](http://archives.datapages.com/data/sepm/journals/v51-54/data/054/054004/1280.htm)
- 317 Dalrymple, R. W., Knight, R., Zaitlin, B. A., & Middleton, G. V. (1990). Dynamics and facies
318 model of a macrotidal sand-bar complex, Cobequid Bay-Salmon River Estuary (Bay of Fundy).
319 *Sedimentology*, 37(4), 577-612.
320 doi: 10.1111/j.1365-3091.1990.tb00624.x
- 321 Dalrymple, R. W., Zaitlin, B. A., & Boyd, R. (1992). Estuarine facies models: conceptual basis and
322 stratigraphic implications: perspective. *Journal of Sedimentary Research*, 62(6), 1130-1146. Retrieved
323 from <http://archives.datapages.com/data/sepm/journals/v59-62/data/062/062006/1130.htm>
- 324 Dalrymple, R. W., & Zaitlin, B. A. (1994). High-resolution sequence stratigraphy of a complex,
325 incised valley succession, Cobequid Bay—Salmon River estuary, Bay of Fundy,
326 Canada. *Sedimentology*, 41(6), 1069-1091.
327 doi: 10.1111/j.1365-3091.1994.tb01442.x
- 328 Dalrymple, R. W., Mackay, D. A., Ichaso, A. A., & Choi, K. S. (2012). Processes,
329 morphodynamics, and facies of tide-dominated estuaries. In: *Principles of Tidal Sedimentology* (Ed. by
330 R.A Davis, R.W Dalrymple and W. Robert), pp. 79-107. Springer Netherlands.
- 331 Davis, R. A., & Hayes, M. O. (1984). What is a wave-dominated coast?. *Marine geology*, 60(1), 313-
332 329.
333 doi: 10.1016/0025-3227(84)90155-5
- 334 Davis, R. A., & Balson, P. S. (1992). Stratigraphy of a North Sea tidal sand ridge. *Journal of*
335 *Sedimentary Research*, 62(1), 116-121. Retrieved from
336 <http://archives.datapages.com/data/sepm/journals/v59-62/data/062/062001/0116.htm>
- 337 Dyer, K. R., & Huntley, D. A. (1999). The origin, classification and modelling of sand banks and
338 ridges. *Continental Shelf Research*, 19(10), 1285-1330.
339 doi: 10.1016/S0278-4343(99)00028-X
- 340 Ehrhold, A., Hamon, D., & Guillaumont, B. (2006). The REBENT monitoring network, a
341 spatially integrated, acoustic approach to surveying nearshore macrobenthic habitats: application
342 to the Bay of Concarneau (South Brittany, France). *ICES Journal of Marine Science: Journal du*
343 *Conseil*, 63(9), 1604-1615.
344 doi: 10.1016/j.icesjms.2006.06.010
- 345 Fichaut, B. (1984). *Réactualisation de la sédimentologie de la rade de Brest* (Doctoral dissertation).
346 Université de Bretagne Occidentale, Brest.
- 347 Garcia-Gíl, S., Durán, R., & Vilas, F. (2000). Side scan sonar image and geologic interpretation of
348 the Ria de Pontevedra seafloor (Galicia, NW, Spain). *Scientia Marina*, 64(4), 393-402.
349 doi: 10.3989/scimar.2000.64n4393

350 Garlan, T. (2012). Deux siècles de cartographie des sédiments marins [Two centuries of marine
351 sediments cartography]. *Revue Le monde des cartes, Bulletin*, 210, 2011-2012.
352 Retrieved from <http://cat.inist.fr/?aModele=afficheN&cpsidt=25935938>

353 Garreau, J. (1980). Structure et relief de la région de Brest [Structure and relief of the Brest
354 area]. *Noroi*, 108(1), 541-548. Retrieved from [http://www.persee.fr/doc/noroi_0029-
355 182x_1980_num_108_1_3925](http://www.persee.fr/doc/noroi_0029-182x_1980_num_108_1_3925)

356 Grall, J., & Hall-Spencer, J. M. (2003). Problems facing maerl conservation in Brittany. *Aquatic
357 Conservation: Marine and Freshwater Ecosystems*, 13(S1), 55-64.
358 doi: 10.1002/aqc.568

359 Grall, J., & Hily, C. (2002). Evaluation de la santé des bancs de maerl de la pointe de Bretagne
360 (*Rapport Direction Régional des Espaces Naturels de Bretagne*). DIREN.

361 Guérin, L. (2004). *La crépidule en rade de Brest: un modèle biologique d'espèce introduite proliférante en réponse
362 aux fluctuations de l'environnement* (Doctoral dissertation). Université de Bretagne occidentale, Brest.

363 Guilcher, A., & Pruleau, M. (1962). Morphologie et sédimentologie sous-marines de la partie
364 orientale de la rade de Brest [Morphology and sedimentology submarine of the eastern part of the
365 Bay of Brest]. *Com. Trav. Hist. Sci., Bull. Sect. Géograph., Géographie de la Mer*, 75, 81-116.

366 Hallégouët, B., Moign, A., Lambert, M.L. (1979). Carte géomorphologique détaillé de la France
367 1:50 000 IV-17, Brest [Detailed geomorphological map of France 1:50 000 IV-17, Brest].
368 Retrieved from <http://bgi-prodig.inist.fr/notice/12718589>

369 Hallégouët, B. (1994). *Formation de la rade de Brest*. In : *Atlas permanent du littoral*, (Ed. by J.-P.
370 Corlaix), pp.22. Editmar.

371 Hinschberger, F., Guilcher, A., Pruleau, M., Moign, A., & Moign, Y. (1968). Carte
372 sédimentologique sous-marine des côtes de France [Submarine sedimentary cartography of the
373 coast of France]. *Feuille de Brest. Echelle, 1*, 100000. Retrieved from
374 http://www.persee.fr/doc/noroi_0029-182182x_1970_num_66_1_1709_t1_0275_0000_1

375 Lamarche, G., Lurton, X., Verdier, A. L., & Augustin, J. M. (2011). Quantitative characterisation
376 of seafloor substrate and bedforms using advanced processing of multibeam backscatter—
377 Application to Cook Strait, New Zealand. *Continental Shelf Research*, 31(2), 93-109.
378 doi: 10.1016/j.csr.2010.06.001

379 Larsonneur, C., Bouysse, P., & Auffret, J. P. (1982). The superficial sediments of the English
380 Channel and its western approaches. *Sedimentology*, 29(6), 851-864.
381 doi: 10.1111/j.1365-3091.1982.tb00088.x

382 Le Chenadec, G. L., Boucher, J. M., & Lurton, X. (2007). Angular Dependence of-Distributed
383 Sonar Data. *Geoscience and Remote Sensing, IEEE Transactions on*, 45(5), 1224-1235.
384 doi: 10.1109/TGRS.2006.888454

385 Lurton, X. (2003). Theoretical modelling of acoustical measurement accuracy for swath
386 bathymetric sonars. *The International hydrographic review*, 4(2), 17-30. Retrieved from
387 <http://cat.inist.fr/?aModele=afficheN&cpsidt=15204452>

- 388 Mazières, A., Gillet, H., Idier, D., Mulder, T., Garlan, T., Mallet, C., ... & Hanquiez, V. (2015).
389 Dynamics of inner-shelf, multi-scale bedforms off the south Aquitaine coast over three decades
390 (Southeast Bay of Biscay, France). *Continental Shelf Research*, 92, 23-36.
391 doi: 10.1016/j.csr.2014.11.002
- 392 Milliman, J. D., Huang-Ting, S., Zuo-Sheng, Y., & Mead, R. H. (1985). Transport and deposition
393 of river sediment in the Changjiang estuary and adjacent continental shelf. *Continental Shelf*
394 *Research*, 4(1), 37-45.
395 doi: 10.1016/0278-4343(85)90020-2
- 396 Moign, Y. (1967). *Contribution à l'Etude Sédimentologique de la Rade et du Goulet de Brest* (Doctoral
397 dissertation). Ecole pratique des hautes études, Dinard.
- 398 Neill, S. P., & Scourse, J. D. (2009). The formation of headland/island sandbanks. *Continental Shelf*
399 *Research*, 29(18), 2167-2177.
400 doi: 10.1016/j.csr.2009.08.008
- 401 Perillo, G. M. (1995). *Geomorphology and sedimentology of estuaries*, 53. Elsevier.
- 402 Robinson, A. H. W. (1960). Ebb-flood channel systems in sandy bays and estuaries. *Geography*,
403 183-199. Retrieved from <http://www.jstor.org/stable/40565158>
- 404 Ryan, D. A., Brooke, B. P., Bostock, H. C., Radke, L. C., Siwabessy, P. J., Margvelashvili, N., &
405 Skene, D. (2007). Bedload sediment transport dynamics in a macrotidal embayment, and
406 implications for export to the southern Great Barrier Reef shelf. *Marine geology*, 240(1), 197-215.
407 doi: 10.1016/j.margeo.2007.02.014
- 408 Service Hydrographique et Océanographique de la Marine, SHOM (1994). *Atlas des courants de*
409 *marée : Courants de marée de la côte Ouest de Bretagne* [Tidal currents of the west Britain coast]
410 (vol. 560).
- 411 Shaw, J., Todd, B.J., & Li, M.Z. (2014). Geologic insights from multibeam bathymetry and
412 seascape maps of the Bay of Fundy, Canada. *Continental Shelf Research*, 83, 53-63.
413 doi: 10.1016/j.csr.2013.12.015
- 414 Tessier, B., Delsinne, N., & Sorrel, P. (2010). Holocene sedimentary infilling of a tide-dominated
415 estuarine mouth. The example of the macrotidal Seine estuary (NW France). *Bulletin de la Societe*
416 *Geologique de France*, 181(2), 87-98.
417 doi: 10.2113/gssgfbull.181.2.87